

## Surface functionalization of polypropylene-bearing isocyanate groups in solid state and their cyclotrimerization with diisocyanates

MengHan Sun,<sup>1</sup> XianMing Zhang,<sup>1</sup> WenXing Chen,<sup>1</sup> LianFang Feng<sup>2</sup>

<sup>1</sup>Key Laboratory of Advanced Textile Materials and Manufacturing Technology, Ministry of Education, Zhejiang Sci-Tech University, Hangzhou, 310018, China

<sup>2</sup>State Key Laboratory of Chemical Engineering, Department of Chemical and Biochemical Engineering, Zhejiang University, Hangzhou, 310027, China

Correspondence to: X. M. Zhang (E-mail: joolizxm@hotmail.com)

**ABSTRACT:** Solid-state graft polymerization of 3-isopropenyl- $\alpha,\alpha'$ -dimethylbenzene isocyanate (TMI) onto the surface of polypropylene beads was carried out in a triethylborane/oxygen redox system. Chemical structures were characterized using attenuated total reflectance–Fourier transform infrared spectroscopy. Results showed that TMI was successfully grafted because of the appearance of an  $\text{—NCO}$  absorption peak at  $2255\text{ cm}^{-1}$ . The emergence of oxygen and nitrogen elements detected by EDS and XPS also demonstrated the existence of isocyanate group on PP-grafted. The grafting ratio of TMI to polypropylene was examined using 9-(methylamino-methyl)anthracene (MAMA) as an intermediate substance. The fluorescent property of MAMA before and after reaction was characterized to guarantee interaction between MAMA and isocyanate. Thermal properties were examined using differential scanning calorimetry–thermogravimetric analysis. Results indicated that melting temperature ( $T_m$ ) of pure PP was  $168^\circ\text{C}$ , while the PP-grafted decreased to  $164^\circ\text{C}$ . Meanwhile, decomposition temperature ( $T_d$ ) decreased with increased grafting ratio for about 8 to  $15^\circ\text{C}$ ; however, when styrene was introduced,  $T_m$  increased probably because of the stabilizing effect on macromolecular radicals and the suppression effect on chain degradation. Besides, the cyclotrimerization of isocyanates on the grafted polymer chain was further conducted to prepare thermally stable isocyanurate composite materials, remedying the  $T_d$  loss of PP-*g*-TMI by improving for  $10^\circ\text{C}$  appropriately. © 2015 Wiley Periodicals, Inc. *J. Appl. Polym. Sci.* **2015**, *132*, 42186.

**KEYWORDS:** crosslinking; grafting; polyolefins; surfaces and interfaces; thermal properties

Received 8 November 2014; accepted 13 March 2015

DOI: 10.1002/app.42186

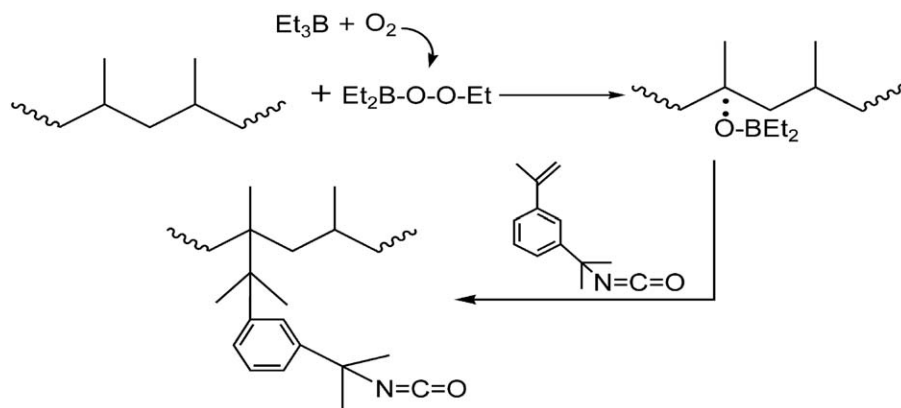
### INTRODUCTION

Polypropylene (PP), which has a linear structure, is one of the most widely used commercial polymer because of its low cost, excellent impact resistance, mechanical toughness, and resistance to chemical attack and aging. However, the low surface energy and high crystallinity of PP lead to poor interfacial adhesion onto other polar materials, which limits its use.<sup>1</sup> Because of these drawbacks, more studies focus on functionalizing PP.<sup>2–6</sup> The functional PP is useful as a kind of compatilizer for blends,<sup>7</sup> composites,<sup>8,9</sup> or as an asphalt modifier.<sup>10,11</sup>

Chemical modification is likely a more practical approach. To attain functionalization, PP is grafted with a vinyl monomer, such as maleic anhydride (MAH)<sup>12,13</sup> and glycidyl methacrylate (GMA),<sup>14,15</sup> and it is processed mainly by molten reaction<sup>16,17</sup> and solution reaction.<sup>18</sup> However, melt reaction is carried out at elevated temperatures, resulting in severe PP degradation, as well as poor thermal and mechanical behaviors.<sup>19,20</sup> Likewise, solution reaction gives off many byproducts to environment,

and the solvents are costly, solvent recycling needs to be done. Solid-phase reaction process is another alternative. It is usually conducted under reduced temperatures, even as low as room temperature. Such conditions reduce possibility of  $\beta$ -scission and lessens degradation of PP.<sup>21,22</sup> By far, PP solid-phase graft polymerization has been researched in various ways by using supercritical carbon dioxide,<sup>23</sup> ball-mixing technique,<sup>24</sup> and solid-state shear pulverization<sup>25,26</sup> and so on.

Functionalization of polymer surface using solid-state graft polymerization is most significant among the other polymerization techniques, which were not feasible in simply modifying particle surfaces. Reports<sup>27,28</sup> had been published about the mechanism of borane/ $\text{O}_2$  radical as a radical initiator. The chemistry involves aerobic oxidation of alkylborane, which forms organoborane peroxide. The borane peroxide then decomposes to borinate radicals, which abstracts tertiary hydrogen of PP chains. The intermediates are formed in situ and finally trapped as adducts into the vinyl monomer. Chung



**Scheme 1.** Mechanism of graft polymerization of TMI onto PP.

*et al.*<sup>29–31</sup> prepared a reversible, controllable active-grafted polymers through injection of oxygen (or air) to alkyl-9-BBN. They studied the inconsistency in phases between borane and oxygen led to a small number of oxidized borane. However, it was sufficient to initiate polymerization.<sup>29</sup> Otherwise, the complexity and availability of Borane/O<sub>2</sub> intermediates was researched as well.<sup>30</sup> Recently, Okamura *et al.*<sup>32</sup> successfully grafted acylic acid, alkyl acrylates, and GMA onto the PP surface to modify its chemical properties.

We grafted a vinyl monomer and obtained a special 3-isopropenyl- $\alpha,\alpha'$ -dimethylbenzene isocyanate (TMI), which contains both a reactive double bond and an isocyanate group. Because of its structure, it was stable enough under processing conditions and was rather unaffected by moisture unlike common isocyanates.<sup>18</sup> Moreover, TMI easily reacts with amine.<sup>33,34</sup> Conversely, it does not react with alcohol and thiol without a catalyst. By selective nucleophilic additions, isocyanates can be used to react with micromolecules-containing amino groups, such as fluorescent MAMA, which may be used to indirectly verify the grafting ratio. PP-g-TMI was a potential material as compatibilizer due to the strongly polar group (–NCO), and the fluorescent derivative was often used to act as a macromolecular tracer during synthesis.<sup>35</sup>

Some comonomers are introduced to improve grafting ratio, such as styrene (St),<sup>15,36</sup> *p*-(3-butenyl)styrene,<sup>37,38</sup> *N*-vinyl pyrrolidone (NVP),<sup>39–41</sup> and so on. They aim to swell the PP surface, stabilize macromolecular radicals and assist bridge effect during grafting. For practicality, researchers selectively incorporate functional groups through post-polymerization in a controlled and mild atmosphere.<sup>42</sup>

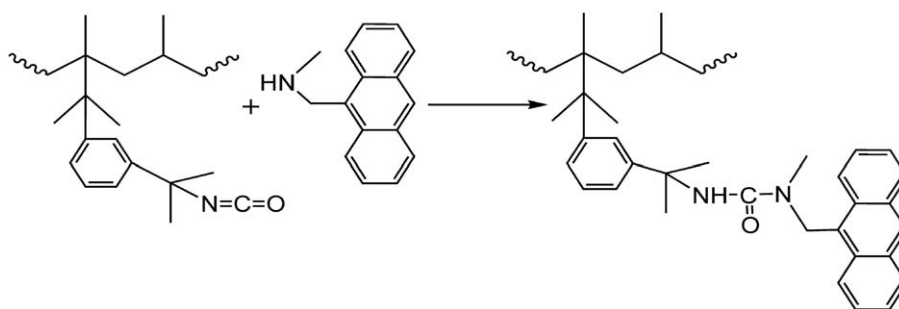
To improve the thermal resistance of PP, three-dimensional network polymers, which consists of thermally stable isocyanurate rings were synthesized; these are promising candidates of high-performance materials.<sup>43</sup> Moritsugu *et al.*<sup>44,45</sup> researched the cyclotrimerization between methylene diphenyl 4,4-diisocyanate (MDI) and propyl isocyanate. In the present study, we investigated the cyclotrimerization of MDI with TMI that is grafted onto PP beads. This process forms protection on the surface that improves the thermal properties.

The article measures grafting ratio improvement based on successful grafting, and its corresponding calculation includes the introduced St. Also, we briefly conducted cyclotrimerization using MDI as the main ingredient. Meanwhile, the thermal properties, fluorescent property, and surface morphology are characterized and analyzed.

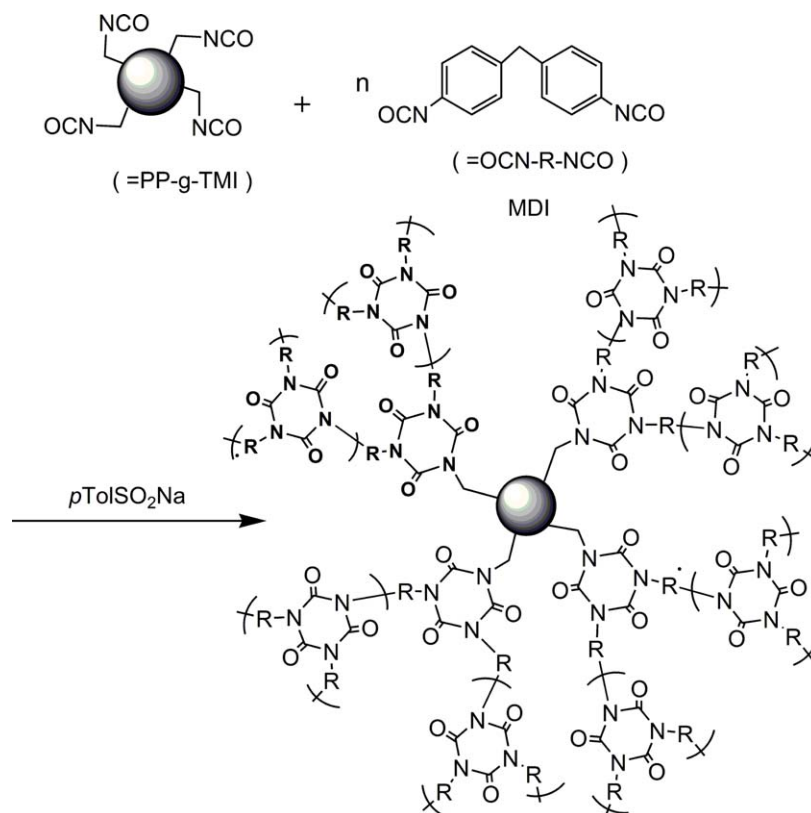
## EXPERIMENTAL

### Materials

PP beads used in this article were of commercial grade (F401) from Nanjing Yangzi Petrochemicals (China). The beads were washed with ethanol and dried at 60°C under reduced pressure before use. A solution of triethylborane (Et<sub>3</sub>B) in THF (1.0M) was purchased from Chengdu Xiya Reagent Research Center (China) and used upon receipt. THF was supplied from Hangzhou Hua-dong Medicine Co., Ltd. (China). TMI monomer and amino MAMA were purchased from J&K Scientific Ltd. MDI (98%), *p*TolSO<sub>2</sub>Na catalyst (98%), and 1,3-dimethyl-2-imidazolidinone (DMI, 98%) solvent were purchased from Aladdin Chemistry Co., Ltd. (USA) and used upon receipt. St was



**Scheme 2.** Mechanism of the synthesis of PP-g-TMI-t-MAMA.



**Scheme 3.** Mechanism of cyclotrimerization of MDI with grafted TMI.

purchased from Tianjin Yong-da Chemical Reagent Co., Ltd. (China) and used after purification, which includes retarder removal, water removal, and reduced-pressure distillation. Acetone was purchased from Zhejiang San-ying Chemical Reagent Co., Ltd. (China) and used upon receipt.

### Measurements

Attenuated total reflectance with Fourier transform infrared (ATR-IR) spectra was obtained using Nicolet 5700 spectrometer equipped with a diamond/ZnSe crystal composite, a range of  $650\text{ cm}^{-1}$  to  $4000\text{ cm}^{-1}$ , a resolution of  $2\text{ cm}^{-1}$ , and a scanning frequency of 64 times. The tested samples were prepared by being pressed into membranes.

The surface elemental analysis via energy X-ray dispersive spectroscopy (EDS) was performed with ULTRATM 55 field-emission scanning electron microscopy operated with an accelerating voltage of 5 kV.

Differential scanning calorimetry (DSC) was performed using Mettler Toledo DSC Analyzer under nitrogen atmosphere. A 4.5 mg sample was initially heated at  $20^\circ\text{C}/\text{min}$  from  $25^\circ\text{C}$  to  $200^\circ\text{C}$ , held at  $200^\circ\text{C}$  for 3 min to remove the residual thermal history, and subsequently cooled at the rate of  $50^\circ\text{C}/\text{min}$  until  $25^\circ\text{C}$ . Then, a second heating proceeded at a heating rate of  $25^\circ\text{C}/\text{min}$ . The melting temperature was obtained from the curve.

Thermal gravimetric analysis (TGA) was determined using Mettler Toledo Thermogravimetric Analyzer. About 8 mg sample was heated from  $25^\circ\text{C}$  to  $600^\circ\text{C}$  with a rate of  $20^\circ\text{C}/\text{min}$  with

constant nitrogen flow. The decomposition temperature was obtained from the curve.

The surface morphology was observed under JSM-5610 scanning electron microscopy at 4 kV acceleration voltage. The samples were dusted with gold before measurement because the polymer had poor electrical conductivity.

The fluorescent property was assessed using Cary 50 UV-VIS continuous spectrophotometer. The fluorescence excitation wavelength was set at 359 nm.

### Free-Radical Graft Polymerization of TMI onto the Surface of PP Beads

Based on the original reference<sup>30,32</sup> on the study of free-radical graft polymerization, the reactions were mainly carried out in a three-

**Table I.** Grafting Ratio of TMI onto PP Beads and Verification of MAMA

Entry	Reaction time (h)	Styrene (mL)	$G_1^a$ (wt %)	$G_2^b$ (wt %)
1	1	0	1.30	1.05
2	1	0.5	1.83	1.35
3	1	2.0	2.80	2.27
4	1	3.0	3.43	3.17
5	3	0	2.43	2.57
6	5	0	2.97	3.06

<sup>a</sup> Grafting ratio calculated according to eq. (1), comprise TMI and St.

<sup>b</sup> Grafting ratio calculated according to eq. (2), comprise TMI.

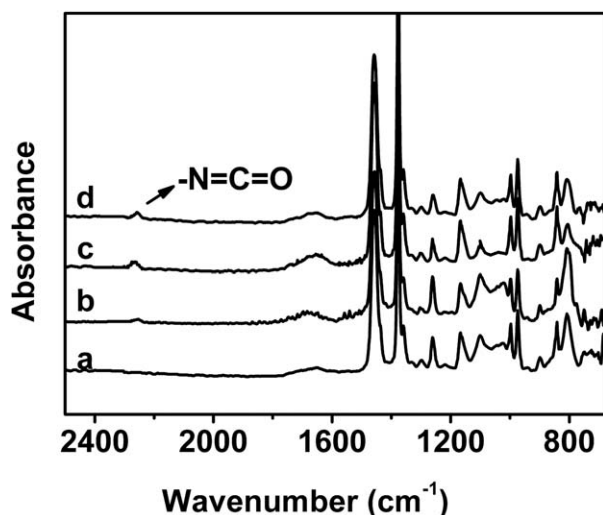


**Figure 1.** ATR-IR spectra of (a) the pure PP beads, (b) PP-g-TMI copolymer with the grafting reaction time of 1 h (Table I, entry 1), (c) PP-g-TMI with 3 h reaction time (Table I, entry 5), and (d) PP-g-TMI with 5 h reaction time (Table I, entry 6).

necked flask and a rotor was gently rotating. Fifteen pieces of PP beads (about 3.0 g) were first placed in the flask and protected under nitrogen atmosphere. After a certain time, a solution of Et<sub>3</sub>B

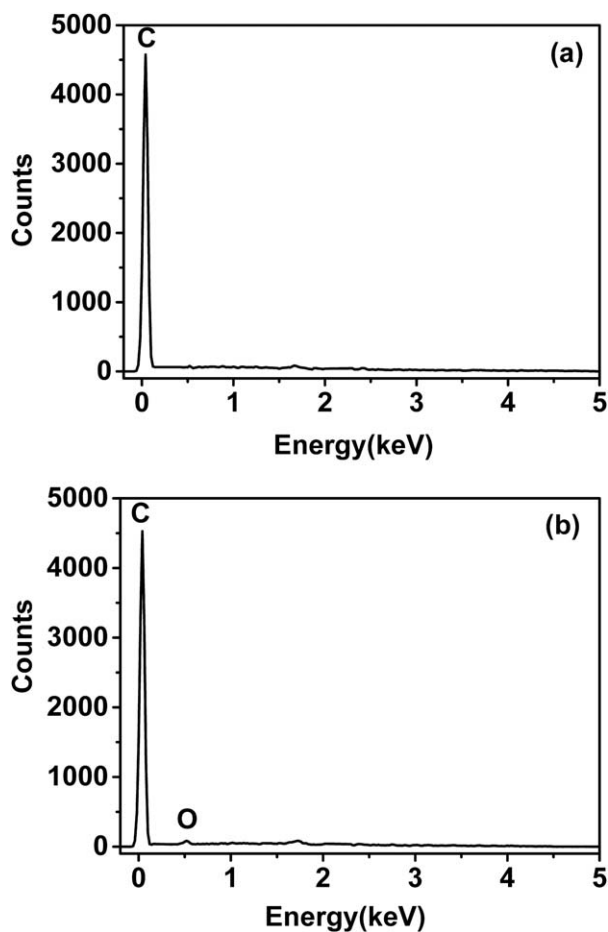


**Figure 2.** EDS spectra of pure PP bead (a) and PP-g-TMI with 5 h reaction time (b).

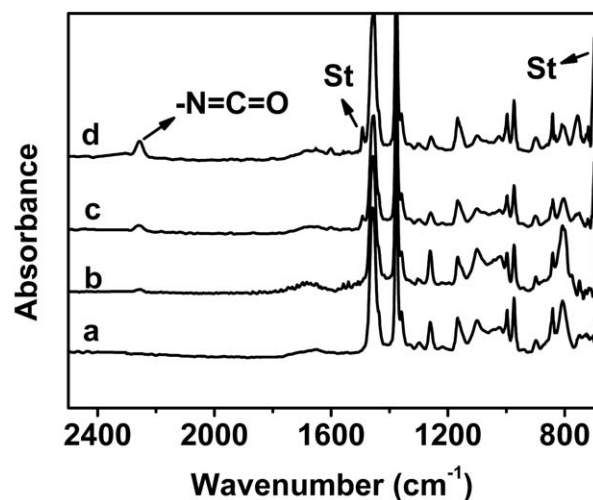


**Figure 3.** ATR-IR spectra of (a) pure PP beads, (b) PP-g-TMI, grafted for 1 h (Table I, entry 1), (c) PP-g-(TMI-t-St) with 2 mL St, grafted for 1 h (Table I, entry 3), and (d) PP-g-(TMI-t-St) with 3 mL St, grafted for 1 h (Table I, entry 4).

in THF (1.0M: 3.0 mL, 3.0 mmol) under nitrogen was added and slowly stirred. Then, 12 h later, the solution was removed using a pipette. The PP beads were placed in a vacuum drying oven for quick drying. The treated PP beads were added with TMI (3 mL, 15.2 mmol) and specific amounts of distilled St by connecting it to the beads under nitrogen atmosphere. Then, a given mass of air was bubbled into the flask under the liquid level. After a fixed time, the resulting products were removed, sonicated, and flushed with acetone for four times, and finally dried under vacuum at 60°C until the weight reached a constant value. The reaction for the synthesis of the grafted material is shown in Scheme 1.

#### Reaction of PP-g-TMI with MAMA to Prepare the Fluorescent Material

Five pieces of grafted PP, obtained from the previous procedure (almost 0.1050 g), were immersed in THF (3.0 mL) at 50°C. A

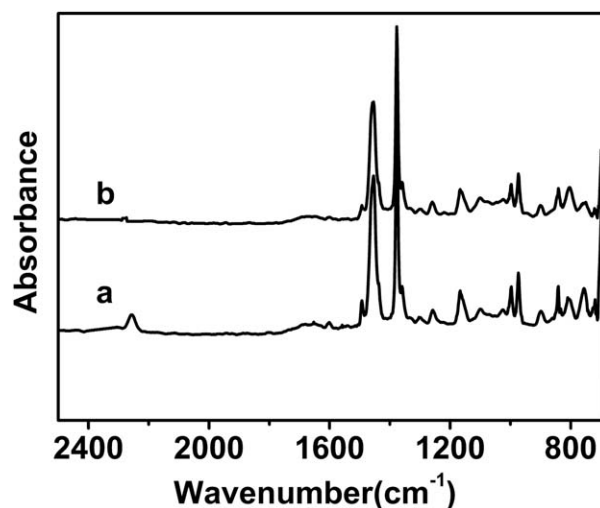


**Figure 4.** ATR-IR spectrum of (a) the starting PP-g-(TMI-t-St) (Table I, entry 4) and (b) the treated PP-g-(TMI-t-St)-MAMA.

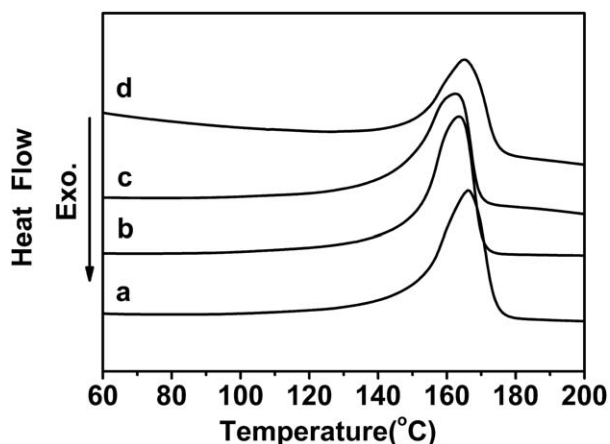


**Figure 5.** DSC curves of (a) the pure PP beads, PP-g-TMI with a reaction time of (b) 3 h (Table I, entry 5) and (c) 5 h (Table I, entry 6), and (d) PP-g-(TMI-t-St) with 3 mL St and 5 h reaction time.

certain amount of MAMA was added into the flask and stirred in a sealed container for 10 h. The obtained PP beads were dried under vacuum at reduced pressure until the mass of the beads became constant. The reaction for the synthesis of PP-g-TMI-t-MAMA is shown in Scheme 2.

#### The Cyclotrimerization of MDI with PP-g-TMI

Five pieces of grafted PP, obtained from the first procedure (about 0.1050 g), were kept under nitrogen atmosphere in a three-necked flask. A well-mixed solution of MDI in DMI (1.0 mL) was initially placed into the flask, and it was followed by *p*TolSO<sub>2</sub>Na (2 mg). After stirring the solution at 50°C for 24 h, the mixture was cooled to room temperature using oil varying. Then, the residue was removed, and the solid particles were sonicated and flushed with acetone for four times and flushed once. Finally, the obtained PP beads were dried at 60°C under vacuum at reduced pressure for 24 h. The cyclotrimerization reaction of MDI with grafted TMI is shown in Scheme 3.

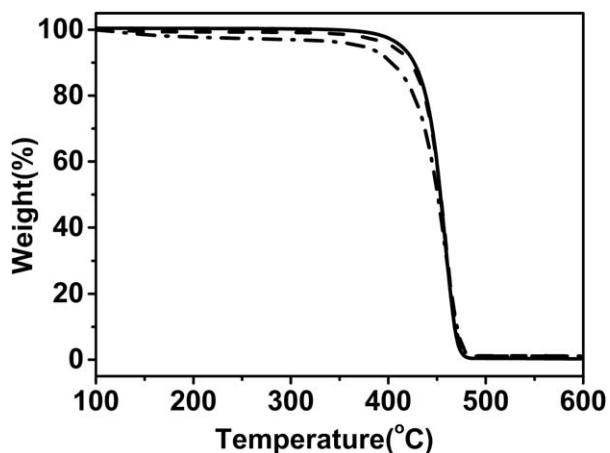


**Figure 6.** TGA curves of pure PP beads (solid line), PP-g-TMI with a reaction time of 1 h (Table I, entry 1) (dashed line), and PP-g-(TMI-t-St) with 3 mL St and a reaction time of 1 h (Table I, entry 4) (dotted-dashed line).

**Table II.** Thermal Stability of Pure and Grafted PP Beads<sup>a</sup>

Sample	$T_{d5}$ (°C)	$T_{d10}$ (°C)
PP	412	426
1-1	404	422
1-4	373	403

<sup>a</sup>The table shows the important values obtained from Figure 6.

#### Calculation of the Grafting Ratio

Based on previous research,<sup>32,46</sup> we used the increase in mass of TMI onto the PP beads to calculate for the grafting ratios. The grafting ratios were verified using the increase in mass of the grafted polymer because of MAMA. Grafting ratios of TMI to PP beads were estimated using the following equation:

$$G_1 = \frac{W_1 - W_0}{W_0} \times 100\% \quad (1)$$

where  $G_1$  is the grafting ratio of TMI,  $W_0$  is the mass of PP beads before grafting, and  $W_1$  is the mass of PP beads after grafting.

The increase in TMI mass was calculated, and the grafting ratios of TMI were verified by introducing MAMA. The equation is as follows:

$$G_2 = \frac{(W_2 - W_1) \times M_1 / M_2}{W_0} \times 100\% \quad (2)$$

where  $G_2$  is the verified grafting ratio of TMI,  $W_2$  is the mass of PP-g-TMI after reacting with MAMA,  $M_1$  is the molar mass of TMI (201.26 g/mol), and  $M_2$  is the molar mass of MAMA (221.30 g/mol).

## RESULTS AND DISCUSSION

### TMI Grafting onto the Surface of PP Beads and Improvement of Grafting Ratios

Table I shows the preparation conditions and the calculated results. The ATR-IR spectrum in Figure 1 indicates an absorption peak at about 2255 cm<sup>-1</sup>, which is attributed to the isocyanate group. It confirms that TMI had been successfully grafted onto the surface of PP beads using Et<sub>3</sub>B/O<sub>2</sub>. As shown in Figure 1, the grafting ratio increases to a small degree as the reaction time increases. This is because the reaction required adequate time to proceed to completion. After 12 h mixed with Et<sub>3</sub>B/THF solution, the surface of PP beads generated a finite amount of reactive borinate macromolecular radicals. As the reaction time increases, transformation of borinate intermediate into PP-g-TMI approaches completion. Besides, the results of EDS analysis shown in Figure 2 revealed after grafting treatment, the percentage of carbon element decreased, while oxygen element appeared. These demonstrated —NCO group was grafted into PP surface indeed, which were in consistency with the results of ATR-IR.

However, the absorption peak of TMI was not as high as that of MAH's as shown in other research.<sup>30</sup> This is because TMI, unlike MAH, cannot self-polymerize but can copolymerize with St. Therefore, we introduced St as the assisting agent to improve the grafting ratio. As shown in Figure 3, the ATR-IR spectra of

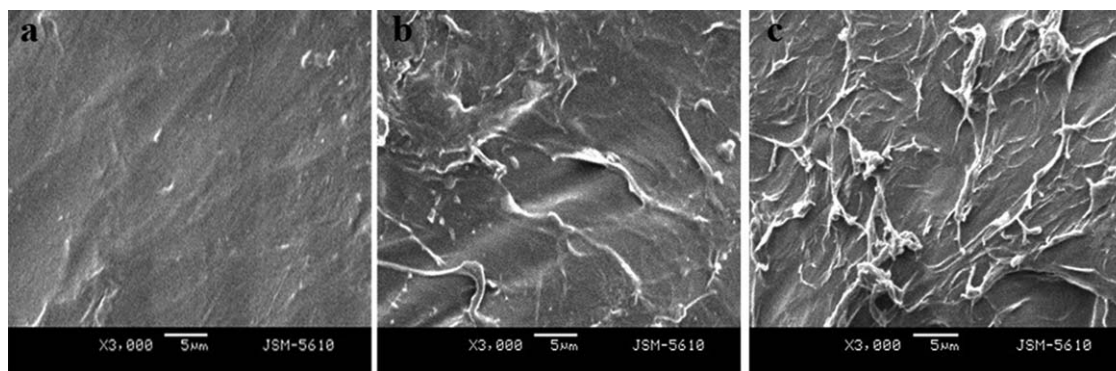


**Figure 7.** SEM photographs of the morphology of (a) pure PP bead, (b) PP bead grafted for 1 h (Table I, entry 1), and (c) PP bead treated with 3 mL St and grafted for 1 h (Table I, entry 4).

the samples that reacted with TMI and St indicate strong absorption at  $2255\text{ cm}^{-1}$ , which is attributed to the isocyanate group of the grafted TMI. The peaks at about  $703\text{ cm}^{-1}$  and  $1495\text{ cm}^{-1}$  are attributed to St  $\nu_{\text{C-H}}$  and  $\nu_{\text{C=C}}$  deformation attached to the benzene ring, respectively. These aforementioned peaks demonstrated that both TMI and St had been grafted onto the bead surface. At the same conditions, higher concentrations of TMI groups were incorporated onto PP with the assistance of St than with TMI alone, which is observable even at a short reaction time (1 h). Increase in the amount of introduced St improved the relative intensity of the isocyanate group at a scope. The effect of St could be confirmed using the melting or solution conditions, which is similar to previous research.<sup>47–49</sup> St, as comonomer, helps in improving the grafting process to a degree which can form the stable macromolecular radicals, preventing the chain scission of PP.

Table I shows the grafting ratios of the samples having different amounts of St at different grafting time. Ratios were calculated using eqs. (1) and (2), and the relative grafting ratios were verified when MAMA was introduced. We obtained similar results between  $G_1$  and  $G_2$  in conditions without St, and the error is within the allowed range. Thus, the method employed in this article, which increased the mass ratio and characterized the

grafting ratios, was feasible. The calculated results were parallel with the conclusions made from the ATR-IR spectra.

Figure 4 shows the ATR-IR spectrum of PP-g-(TMI-t-St) and PP-g-(TMI-t-St)-MAMA. It indicates that the absorption peak of isocyanate almost disappeared, which demonstrated that  $-\text{NCO}$  had been largely consumed by MAMA. Hence, it simply confirmed that increasing the mass through MAMA reaction with isocyanate was preferred.

#### Characterizations of Thermal Properties, Surface Morphology, and Fluorescence

The thermal stability of the polymer beads, before and after treatment, was analyzed using DSC/TGA. Figure 5 compares the four DSC curves of pure PP beads, PP-g-TMIs with different reaction times (3 h and 5 h), and PP-g-(TMI-t-St) with 3 mL St and 5 h reaction time.  $T_m$  of pure PP beads at a heating rate of  $25^\circ\text{C}/\text{min}$  was almost  $168^\circ\text{C}$ .  $T_m$ s of PP-g-TMIs with different reaction times were identical at approximately  $164^\circ\text{C}$ .  $T_m$  of the PP-modified has declined from the pure PP beads. This may be due to the grafted TMI short chains that form a disordered branched structure, which destroyed the uniform molecular structure of PP chains.<sup>50,51</sup> The degradation of the polymer

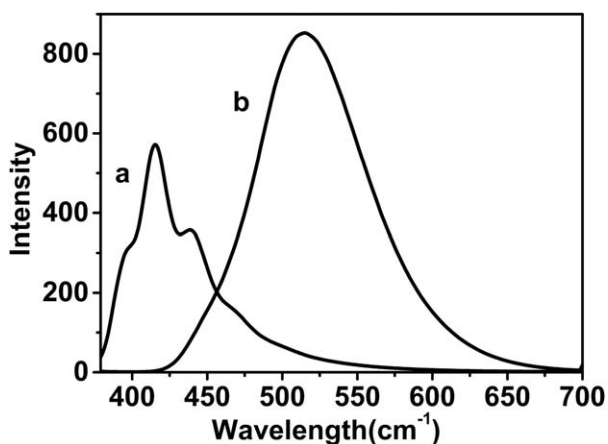


**Figure 8.** Fluorescence spectrum of (a) PP-g-TMI-MAMA and (b) pure MAMA.

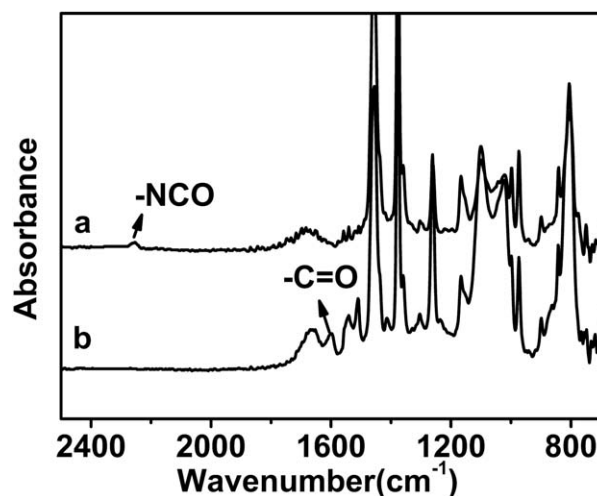


**Figure 9.** ATR-IR spectrum of (a) PP-g-TMI with a reaction time of 3 h (Table I, entry 5) and (b) the network polymer of cyclotrimerization of MDI (75 mg) with grafted TMI.

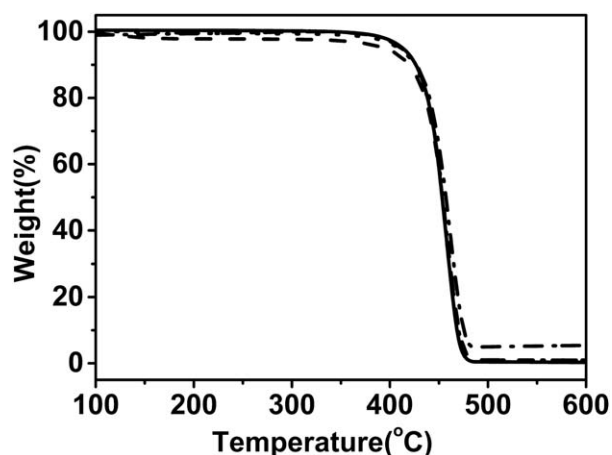


**Figure 10.** TGA curves of pure PP beads (solid line), PP-g-TMI with a reaction time of 3 h (dashed line), and the network polymer of cyclotrimerization of grafted TMI with 25 mg MDI (dotted line) and 75 mg MDI (dotted–dashed line).

chains during PP modification was also one of the reasons. As St was introduced into the grafting system,  $T_m$  is slightly higher compared with samples grafted with TMI only. Hence, St stabilized the macromolecular radicals and prevented the PP chains from degradation.

As shown in Figure 6, the decomposition of the beads was based on TGA curves with temperature ranging from 100°C to 600°C. The corresponding  $T_{d5}$  and  $T_{d10}$  (decomposition temperatures at 5% and 10% weight loss, respectively) are listed in Table II. The resulting grafted copolymers exhibited lower thermal stability than the pure PP beads. PP-modified polymers are more likely decomposed at lower temperatures. This can be attributed to the unstable grafted monoisocyanate that deteriorated PP chains. Moreover,  $T_{d5}$  and  $T_{d10}$  lowered as the content of monoisocyanate increased.

The morphology of the surfaces of PP beads with protective gold coating is shown in Figure 7. Apparently, pure PP bead presented a smooth surface at high magnification. The PP-g-TMI bead with a grafting ratio of 1.30% revealed an uneven surface because of the grafted branches. Figure 7(c) shows that more gibbous structures were formed on the surface of PP-g-(TMI-t-St) as compared with that of PP-g-TMI in Figure 7(b). Larger and denser tentacles were observed on the surface of PP-g-TMI than that of pure PP beads shown in Figure 7(a). The SEM images gave the evidence that the grafting ratio increased. However, the irregular distribution of the grafting was observed.

Figure 8 shows the fluorescence spectrum of MAMA before and after the reaction of the grafted TMI with MAMA. Fluorescence excitation wavelength was set at 359 nm, and the fluorescence spectra from 375 nm to 700 nm was obtained. Within the said range, PP and PP-g-TMI did not show any peak and thus, it is not fluorescent. The only spectra that shows strong peaks are those with pure MAMA at 512 nm, which is a broad peak, and the polymer that is reacted with MAMA, which has three characteristic peaks at 396, 415, and 440 nm. Because the concentra-

**Table III.** Thermal Stability of the Network Polymer of Cyclotrimerization of Grafted TMI with Different Amounts of MDI<sup>a</sup>

Sample	M(MDI) (mg)	$T_{d5}$ (°C)	$T_{d10}$ (°C)
1–5	0	395	419
1	25	415	429
2	75	414	428

<sup>a</sup>The table shows the important values obtained from Figure 10.

tion of the reacted MAMA was low, the conspicuous distinction among the loops in anthracene are observed. Moreover, a hypsochromic shift is caused by a mutual reaction between  $-\text{NCO}$  and  $-\text{NH}_2$  that resulted in the increase of fluorophore hydrophobicity and in the decrease of polarity.<sup>52</sup>

### Cyclotrimerization of MDI with Grafted TMI and its Thermal Stability

As shown in Figure 9, after the cyclotrimerization of PP-g-TMI with MDI, the absorption peak at  $2255\text{ cm}^{-1}$  became negligible. This implied that the isocyanates were almost consumed. The absorption that appeared at about  $1600\text{ cm}^{-1}$  is attributed to carbonyl stretching vibration in the six-membered ring, based on the fact that isocyanate groups were depleted, and the networked structure was formed. In addition, the strength of carbonyl absorption was much stronger than that of isocyanate because after cyclotrimerization, the concentration of the formed  $-\text{C}=\text{O}$  was higher than the initially grafted TMI.

After ATR-IR analysis, the products of cyclotrimerization were then analyzed using TGA in investigating their thermal stability. Figure 10 and Table III shows the resulting thermographs.  $T_{d5}$  of the networked polymer was approximately 414°C, and the TGA curve is smooth. This showed good heat resistance without significant decomposition before reaching 410°C. At approximately 450°C, the rate of decomposition is at its maximum. When the temperature reached 490°C, the curve plateaued, which means that the decomposition ended. Compared with grafted PP, networked polymer has about 10°C higher  $T_d$ . The weight loss of networked polymer consisting of high-concentration MDI remained at 5%, whereas other samples reached zero at the same elevated temperature. This demonstrated that cyclotrimerization improved the thermal stability of PP at a certain degree, as compared with the grafted PP.

### CONCLUSIONS

In this article, a novel method in grafting TMI onto the surface of PP beads was conducted using  $\text{Et}_3\text{B}/\text{O}_2$ . Reaction of  $-\text{NCO}$  with  $-\text{NH}_2$  was also applied to verify the amount of the grafted TMI. Free-radical polymerization was conducted using the solid-state raw material, which reduced the possibility of PP degradation comparing with the melting method. ATR-IR indicated the absorption peak of the grafted functional group  $-\text{NCO}$ , which appeared at  $2255\text{ cm}^{-1}$ . This revealed that TMI had been grafted onto PP successfully. Based on the values calculated using eqs. (1) and (2), the grafting ratios increased as the reaction time is increased because of the degree at which the reaction approaches completion. Moreover, introduction of

St, as a comonomer, stabilized macromolecular radicals, which is assumed to be responsible for promoting grafting levels. The  $T_m$  and  $T_d$  were both partially affected by the grafting ratios of PP. The surface of grafted PP beads was much more uneven than pure PP surface. As PP-functionalized, the grafted —NCO groups are potential to improve low surface energy of PP to achieve better adhesion property, and PP-g-TMI-MAMA can be used to act as a macromolecular tracer during synthesis. Finally, the networked polymer designed was highly effective and selective during cyclotrimerization of isocyanates between MDI and the grafted TMI. It also showed improved thermal stability in PP-g-TMI, whereas the thermal stability in pure PP beads was conserved. Here, the article focused on the elementary researches, so that the properties of modified PP membrane and fiber are needed further practical consideration.

#### ACKNOWLEDGMENTS

The authors thank the National Natural Science Foundation of China (Grant No. 51103135), the Zhejiang Provincial Natural Science Foundation of China (Grant No. Y4100534), and Zhejiang Provincial Pandeng Plan of China (pd2013129) for their financial support.

#### REFERENCES

1. Rätzsch, M.; Arnold, M.; Borsig, E.; Bucka, H.; Reichelt, N. *Prog. Polym. Sci.* **2002**, *27*, 1195.
2. Passaglia, E.; Coiai, S.; Augier, S. *Prog. Polym. Sci.* **2009**, *34*, 911.
3. Song, Y. Q.; Sheng, J.; Wei, M.; Yuan, X. B. *J. Appl. Polym. Sci.* **2000**, *78*, 979.
4. Ma, H. M.; Davis, R. H.; Bowman, C. N. *Macromolecules* **2000**, *33*, 331.
5. Yovcheva, T. A.; Avramova, I. A.; Mekishev, G. A.; Marinova, T. S. *J. Electrostat.* **2007**, *65*, 667.
6. Haldar, S. K.; Singha, N. K. *J. Appl. Polym. Sci.* **2006**, *101*, 1340.
7. Lin, Z.; Guan, Z.; Xu, B.; Chen, C.; Guo, G.; Zhou, J.; Xian, J. M.; Cao, L.; Wang, Y. L.; Li, M. Q.; Li, W. *J. Ind. Eng. Chem.* **2013**, *19*, 692.
8. Thakur, V. K.; Vennerberg, D.; Kessler, M. R. *Appl. Mater. Interfaces* **2014**, *6*, 9349.
9. Manias, E.; Touny, A.; Wu, L.; Strawhecker, K.; Lu, B.; Chung, T. C. *Chem. Mater.* **2001**, *13*, 3516.
10. Hong, M.; Cui, L.; Liu, S.; Li, Y. *Macromolecules* **2012**, *45*, 5397.
11. Hong, M.; Liu, J. Y.; Li, B. X.; Li, Y. S. *Macromolecules* **2011**, *44*, 5659.
12. Lu, B.; Chung, T. C. *Macromolecules* **1998**, *31*, 5943.
13. Shi, D.; Yang, J. H.; Yao, Z. H.; Wang, Y.; Huang, H. L.; Jing, W.; Yin, J. H.; Costa, G. *Polymer* **2001**, *42*, 5549.
14. Pracella, M.; Chionna, D. *Macromol. Symp.* **2003**, *198*, 161.
15. Li, J. L.; Xie, X. M. *Polymer* **2012**, *53*, 2197.
16. Huang, H.; Liu, N. C. *J. Appl. Polym. Sci.* **1998**, *67*, 1957.
17. Dorscht, B. M.; Tzoganakis, C. *J. Appl. Polym. Sci.* **2003**, *87*, 1116.
18. Hu, G. H.; Li, H. X.; Feng, L. F.; Luiz, A. P. *J. Appl. Polym. Sci.* **2003**, *88*, 1799.
19. Kruse, T. M.; Wong, H. M.; Broadbelt, L. T. *Macromolecules* **2003**, *36*, 9594.
20. De Roover, B.; Sclavons, M.; Carlier, V.; Devaux, J.; Legras, R.; Momtaz, A. *J. Polym. Sci. Part A: Polym. Chem.* **1995**, *33*, 829.
21. Qiu, W. L.; Takahiro, H. *Macromol. Chem. Phys.* **2005**, *206*, 2470.
22. Smith, A. P.; Shay, J. S.; Spontak, R. J.; Balik, C. M.; Ade, H.; Smith, S. D.; Koch, C. C. *Polymer* **2000**, *41*, 6271.
23. Zhang, A. F.; Zhang, Z. Y.; Gong, Y. F. *Acta Polym. Sin.* **2004**, *2*, 292.
24. Qiu, W. L.; Zhang, F. R.; Takashi, E.; Takahiro, H. *J. Appl. Polym. Sci.* **2003**, *91*, 1703.
25. Diop, M. F.; Torkelson, J. M. *Polymer* **2013**, *54*, 4143.
26. Diop, M. F.; Torkelson, J. M. *Macromolecules* **2013**, *46*, 7834.
27. Sonnenschein, M. F.; Webb, S. P.; Kastl, P. E.; Arriola, D. J.; Wendt, B. L.; Harrington, D. R.; Rondan, N. G. *Macromolecules* **2004**, *37*, 7974.
28. Hong, H.; Chung, T. C. *Macromolecules* **2004**, *37*, 6260.
29. Chung, T. C.; Janvikul, W.; Lu, H. L. *J. Am. Chem. Soc.* **1996**, *118*, 705.
30. Wang, Z.; Hong, M. H.; Chung, T. C. *Macromolecules* **2005**, *38*, 8966.
31. Dong, J. Y.; Manias, E.; Chung, T. C. *Macromolecules* **2002**, *35*, 3439.
32. Okamura, H.; Sudo, A.; Endo, T. *J. Polym. Sci. Part A: Polym. Chem.* **2009**, *47*, 6163.
33. Zhu, S. Y.; Zhang, X. M.; Chen, W. X.; Feng, L. F. *Polym. Compos.* **2015**, *36*, 482.
34. Zhu, S. Y.; Li, H.; Zhang, X. M.; Chen, W. X.; Feng, L. F. *Des. Monomers Polym.* **2015**, *18*, 232.
35. Zhang, X. M.; Zhu, S. Y.; Zhang, C. L.; Feng, L. F.; Chen, W. X. *Polym. Eng. Sci.* **2014**, *54*, 310.
36. Cartier, H.; Hu, G. H. *J. Polym. Sci. Part A: Polym. Chem.* **1998**, *36*, 1053.
37. Zhang, Z. J.; Wan, D.; Xing, H. P.; Zhang, Z. J.; Tan, H. Y.; Wang, L.; Zheng, J.; An, Y. J.; Tang, T. *Polymer* **2012**, *53*, 121.
38. Wan, D.; Xing, H. P.; Wang, L.; Zhang, Z. J.; Qiu, J.; Zhang, G. C.; Tang, T. *Polymer* **2013**, *54*, 639.
39. Yang, H. W.; Luan, S. F.; Zhao, J.; Shi, H. C.; Li, X. M.; Song, L. J.; Jin, J.; Shi, Q.; Yin, J. H.; Shi, D.; Stagnaro, P. *Polymer* **2012**, *53*, 1675.
40. Jin, J.; Zhang, C.; Jiang, W.; Luan, S. F.; Yang, H. W.; Yin, J. H.; Stagnaro, P. *Colloids Surf. A* **2012**, *407*, 141.
41. Yang, H. W.; Luan, S. F.; Zhao, J.; Shi, H. C.; Shi, Q.; Yin, J. H.; Stagnaro, P. *React. Funct. Polym.* **2010**, *70*, 961.
42. Boalen, N. K.; Hillmyer, M. A. *Chem. Soc. Rev.* **2005**, *34*, 267.
43. Samborska-Skowron, R.; Balas, A. *Polym. Adv. Technol.* **2002**, *13*, 653.



44. Moritsugu, M.; Sudo, A.; Endo, T. *J. Polym. Sci. Part A: Polym. Chem.* **2011**, *49*, 5186.
45. Moritsugu, M.; Sudo, A.; Endo, T. *J. Polym. Sci. Part A: Polym. Chem.* **2012**, *50*, 4365.
46. Zhu, B. D.; Dong, W. C.; Wang, J.; Song, J.; Dong, Q. *J. Appl. Polym. Sci.* **2012**, *126*, 1844.
47. Kim, J.; Lee, J.; Son, Y. *Mater. Lett.* **2014**, *126*, 43.
48. Wan, D.; Ma, L.; Xing, H.; Wang, L.; Zhang, Z.; Qiu, J.; Zhang, G. C.; Tang, T. *Polymer* **2013**, *54*, 639.
49. Li, H.; Zhang, X. M.; Zhu, S. Y.; Chen, W. X.; Feng, L. F. *Polym. Eng. Sci.* **2014**, *55*, 614.
50. Wang, L.; Yang, H. F.; Tan, H. Y.; Yao, K.; Gong, J.; Wan, D.; Qiu, J.; Tang, T. *Polymer* **2013**, *54*, 3641.
51. Mousavi-Saghandikolaei, S. A.; Frounchi, M.; Dadbin, S.; Augier, S.; Passaglia, E.; Ciardelli, F. *J. Appl. Polym. Sci.* **2007**, *104*, 950.
52. Valeur, B.; Leray, I. *Coord. Chem. Rev.* **2000**, *205*, 3.